Journal of Assisted Reproduction and Genetics (2025) 43:293–306
https://doi.org/10.1007/s10815-025-03721-0

REPRODUCTIVE PHYSIOLOGY AND DISEASE

Age-related changes in mitochondrial markers and telomere dynamics during initial growth of human preantral follicles

Luciana Cacciottola[1] · Manyu Zhang[1] · Lara Houeis[1] · Caroline Bouzin[2] · Marie-Astrid van Dievoet[3] · Mathieu Luyckx[4] · Jacques Donnez[5,6] · Marie-Madeleine Dolmans[1,4]

Received: 12 June 2025 / Accepted: 6 October 2025 / Published online: 25 October 2025

Abstract

Purpose To investigate how mitochondria and telomeres evolve during early follicle growth in human preantral follicles, and how these changes relate to reproductive age.

Methods This prospective study included ovarian cortex and peripheral blood samples from 21 women, categorized into young (20–26, $n=7$), mid (27–36, $n=6$) and advanced (37–46, $n=8$) reproductive age groups. Ovarian biopsies were processed for (i) follicle isolation for mitochondrial marker assessment (MitoTracker Deep Red and MitoSOX live staining) and telomerase subunit expression (*hTERT, hTERC*) by droplet digital PCR; and (ii) histological evaluation of the ovarian follicle pool, mitochondrial mass (TOMM20) and telomere length in different ovarian compartments (oocytes, granulosa cells and stroma) by fluorescence in situ hybridization (FISH). Leukocyte telomere length was measured by flow-FISH.

Results Mitochondrial mass (TOMM20) in the follicle pool was stable across age groups, but increased significantly during early follicle growth in younger patients ($p<0.01$). Active mitochondria did not decline with age, but reactive oxygen species (ROS) generation showed complex age-related patterns, with younger subjects exhibiting lower ROS levels during follicle growth ($p<0.01$) than other age groups. Telomere length was stable in granulosa cells and oocytes within primordial follicles, but increased during growth in younger age groups. Telomerase subunit expression was detected in preantral follicles without any significant age or size differences.

Conclusions These results point to greater mitochondrial mass, mitochondrial ability to limit ROS generation, and telomere dynamics changing with increasing age in early growing follicles, potentially guiding the development of strategies to enhance fertility outcomes during the early stages of folliculogenesis.

Keywords Ovarian aging · Fertility · Mitochondria · Follicle isolation · Telomere length · Telomerase

Introduction

Infertility is emerging as one of the greatest challenges ever faced in human reproduction, affecting up to one in four couples around the world. A number of aspects have been instrumental in these over recent decades. One is maternal

The authors Luciana Cacciottola and Manyu Zhang have contributed equally as first authors.

✉ Marie-Madeleine Dolmans
marie-madeleine.dolmans@uclouvain.be

1 Gynecology Research Unit, Institut de Recherche Expérimentale Et Clinique, Université Catholique de Louvain, Avenue Mounier 52, Bte. B1.52.02, Brussels 1200, Belgium

2 2IP-IREC Imaging Platform (RRID:SCR_023378), Institute of Experimental and Clinical Research, Université Catholique de Louvain, Brussels, Belgium

3 Hematology Department of Laboratory Medicine, Cliniques Universitaires Saint-Luc, Brussels, Belgium

4 Gynecology Department, Cliniques Universitaires Saint-Luc, Brussels, Belgium

5 Society for Research Into Infertility, Brussels, Belgium

6 Université Catholique de Louvain, Brussels, Belgium

age, which is increasing due to women postponing childbearing until their later years on account of changes in their role and rights in modern society [1, 2]. Ovarian function and somatic aging appear to be closely connected, the age of menopause being an important indicator of quality of life and overall life expectancy in women [3]. However, aging at the cellular level cannot be generalized to all organs, and mechanisms responsible for ovarian cell senescence appear to have their own specific regulation, which also may differ between somatic and germ cells. Moreover, a number of external and individual factors, including metabolic status, endocrine and inflammatory conditions and lifestyle habits, can further modulate ovarian aging and influence mitochondrial and telomere dynamics [4, 5].

The ovarian reserve continues to decrease in size over the course of the reproductive lifespan, accompanied by a reduction in the quality of remaining oocytes, leading to impaired ovulation or embryo alterations, like a higher risk of aneuploidy [5]. Optimal oocyte maturation depends on intrinsic factors, namely fully functioning cell machinery, but also extrinsic factors, such as granulosa cells (GCs) providing a nutrient supply, sustaining steroidogenesis and scavenging discarded products [6, 7]. One of the most commonly described age-related impairments in oocytes involves molecular mechanisms ensuring genomic stability, including telomere shortening, reduced expression of cohesin complex proteins responsible for accurate chromosome segregation, altered DNA repair pathways and epigenetic modifications, such as histone deacetylation and aberrant DNA methylation [4]. Some of these mechanisms are also shared with surrounding somatic cells, particularly GCs, which undergo specific epigenetic regulation. Cumulus GCs obtained during oocyte retrieval for assisted reproductive techniques (ART) show specific epigenetic regulation, like decreased methylation [8] and longer telomeres than peripheral leukocytes [9, 10]. Indeed, they correlate poorly with chronological age when tested against various epigenetic clocks [4]. Nevertheless, major changes in these parameters, like critically short telomeres that fail to maintain chromosomal endprotection, as well as accumulation of telomere-associated DNA damage foci, have been linked to increased senescence, reduced proliferative capacity and altered steroidogenic function in GCs [11, 12]. These telomeric alterations are associated with a diminished ovarian reserve and poor fertility outcomes [4, 8–12].

Another key cell function involved in ovarian aging is the actual mitochondrial machinery that sustains metabolic activity in oocytes and their surrounding GCs [13]. Mitochondrial biogenesis starting with mitochondrial DNA expansion is crucial for oocyte maturation, fertilization and embryo development [14]. Impaired mitochondrial function and biogenesis were observed in women with advanced reproductive age or a diminished ovarian reserve [15, 16]. Such impairment limits the energy supply available for follicle growth and maturation, while increasing oxidative stress and cell damage due to imbalanced reactive oxygen species (ROS) production [5, 6, 17].

Almost all our knowledge of these cell function regulations in humans comes from ART studies analyzing oocytes and cumulus GCs at ovulation, namely at the end of their maturation path. However, these investigations are typically conducted in the specific context of infertility and ovarian stimulation, which may offer only a partial view of the physiological behavior of these markers. Much less is known about how these age-related cell functions behave in the preantral follicle pool during primordial follicle (PF) activation and initial growth. According to the mitochondrial bottleneck theory reported by several authors [13], PFs in mammals preserve a minimal, mutation-free mitochondrial pool that expands upon activation [13, 18]. In mouse models, mitochondrial biogenesis has been observed at early follicle stages, with transmission electron microscopy (TEM) revealing reduced mitochondrial coverage, and mtDNA quantification indicating decreased biogenesis in the preantral follicle pool with increasing age [19]. In humans, isolated preantral follicles from the ovarian cortex of prepubertal subjects were shown to have more mitochondria in a less active state than adult subjects. Moreover, their morphology and distribution in oocytes, assessed by TEM, were also found to vary before and after puberty [20].

Altered mitochondrial function disrupts chromosome segregation and may contribute to genetic instability. Mitochondria and telomeres are interconnected through a bidirectional regulatory axis, wherein mitochondrial dysfunction can trigger oxidative stress that accelerates telomere attrition, while telomere damage can in turn provoke p53-dependent repression of mitochondrial biogenesis promoter PGC-1α. This impairs mitochondrial biogenesis and function [21–23]. Telomere dynamics, however, remain largely unexplored in the distinct cellular compartments of the human ovarian cortex. Since PFs remain quiescent for decades in ovarian tissue, understanding how early biological processes are regulated during initial follicle growth is key to identifying the earliest cellular signs of ovarian aging. Mitochondrial integrity and telomere stability are two critical markers known to influence oocyte quality and are often compromised with advancing reproductive age. This study was designed to investigate whether these cellular features show age-related alterations in the quiescent follicle pool and whether they are further affected during early follicle growth. Samples from a representative cohort of women with an age range covering the entire reproductive lifespan were used.

Materials and methods

Experimental design

Use of human ovarian tissue and blood samples was approved by the Institutional Review Board of the Université Catholique de Louvain (2012/23MAR/12500). Samples (ovarian tissue biopsies and peripheral blood samples) were obtained after obtaining written informed consent from 21 women (20–46 years) after surgery for benign gynecological conditions. Seven patients had endometriosis (either infiltrating deep into the recto-vaginal space or peritoneal), four were undergoing tubal surgery (salpingectomy or salpingoneostomy), and 9 presented with uterine indications like fibroids and/or heavy menstrual bleeding (Supplementary Information 1). Women with ovarian pathologies like ovarian endometriosis and/or a history of infertility were excluded. The rationale for patient selection was to avoid including subjects who may have shown pre-existing alterations in the biological parameters under investigation. Blood samples were acquired for flow fluorescence in situ hybridization (flow-FISH) on the same day as surgery to investigate telomere length in leukocytes. Patients were stratified into three reproductive age groups based on changes in the preantral follicle cohort: young (20–26 years), mid (27–36 years) and advanced (37–46 years).

Ovarian cortical strips were kept on ice in minimal essential medium (MEM) plus Glutamax (Gibco, Invitrogen, Belgium) until they reached the laboratory. One fragment of around 4 × 3 × 2 mm was used for histological analyses to assess mitochondrial mass (TOMM20 by immunohistochemistry [IHC]) and telomere length by FISH. Another fragment, ranging from 5 × 5 × 2 mm to 5 × 10 × 2 mm in size depending on tissue availability, was further processed for follicle isolation to assess mitochondrial markers using two fluorogenic dyes (MitoTracker Deep Red and MitoSOX) for live cell staining. When available, the remaining ovarian tissue was cryopreserved by slow freezing for further analysis to evaluate the expression of *hTERT* and *hTERC* telomerase subunits by droplet digital PCR (ddPCR). Patient characteristics and numbers of isolated follicles allocated to different analyses are shown in Supplementary Information 1.

Telomere length assessment in peripheral leukocytes

Telomere length in leukocytes was measured by flow-FISH at Cliniques Universitaires Saint Luc, as previously established [24]. Briefly, after red blood cell lysis with ammonium chloride, white blood cells were frozen at − 80 °C until analysis. Bovine thymocytes were mixed with each sample as internal control cells. A fluorescein isothiocyanate (FITC)-labeled peptide nucleic acid (PNA) probe was added to stain telomeres, before calculating the fluorescent signal using a Navios EX flow cytometer (Beckman Coulter).

Follicle isolation

Ovarian cortex was mechanically minced into fragments with a tissue chopper (McIlwain Tissue Chopper, Mickle Laboratory, Guildford, UK) and incubated in 10 mL Dulbecco's phosphate-buffered saline (PBS) with Ca2 + and Mg2 + (Gibco, Thermo Fisher Scientific, Ghent, Belgium). This was done in the presence of 0.28 Wünsch units/mL Liberase DH (Roche Diagnostics) and 8 Kunitz units/mL DNase I (Roche Diagnostics, Brussels, Belgium) in a water bath (37 °C) for 30 min with gentle shaking and pipetting every 15 min. After 30 min, the suspension was filtered through a 100-µm cell strainer (Imtec, Germany), then a 30-µm strainer (Imtec, Germany), after being inactivated with the same volume of PBS plus 10% heat-inactivated fetal bovine serum (HIFBS). The enzymatic digestion step was repeated with ovarian tissue fragments collected from the 100-µm cell strainer, while isolated follicles from the 30-µm filter were recovered by washing the nylon mesh in 3 mL PBS + 10% HIFBS. Undigested fragments were subjected to the same procedure twice more (at 60 and 90 min) until complete tissue digestion [25]. Fully isolated follicles were retrieved with the help of a stereomicroscope and a 130-µm micropipette by two operators and placed in PBS plus 10% HIFBS medium at 4 °C.

Histological ovarian reserve evaluation

Cortical fragments were fixed in 4% formaldehyde, embedded in paraffin and cut into 5-µm sections. Hematoxylin and eosin (H&E) were used to stain every sixth slide to determine follicle count and classification, while sections in between were prepared for IHC and FISH. Six random H&E-stained sections per sample were digitized using the Pannoramic P250 Flash III slide scanner (3DHistech, Hungary), then closely examined using CaseViewer (v2.3). Follicles with a visible oocyte were counted and classified according to developmental stage into PFs (including both primordial and transitory follicles) and growing follicles (GFs) (including primary and secondary follicles). Atretic follicles were evaluated in line with specific morphological criteria, including (i) ooplasm eosinophilia, (ii) GC pyknosis or (iii) cytoplasmic contraction [26]. Follicle density was expressed as the number of follicles per mm^3.

Ovarian tissue freezing and thawing

Surplus cortical strips from six subjects were cryopreserved by a slow-freezing protocol and thawed following established procedures [27]. Briefly, cortical fragments were immersed in freezing medium composed of 10% dimethyl sulfoxide (DMSO) (Sigma, Belgium), placed in a programmable freezer (Kryo 10, Series III, Planer, UK) and then stored in liquid nitrogen. For thawing, they were kept at room temperature for 2 min, immersed in a water bath at 37 °C for another 2 min, then washed 3 times in fresh MEM plus Glutamax (Gibco, Invitrogen, Belgium).

Mitochondrial evaluation

1. Mitochondria and mitochondrial ROS labeling in isolated follicles

Mitochondrial parameters in isolated follicles were investigated using 2 fluorescent probes: MitoTracker Deep Red (Invitrogen M46753, Belgium) and MitoSOX Red (Invitrogen M36008, Belgium). The first enables active mitochondria visualization, while the second targets anion superoxide of mitochondrial origin in live cells.

Isolated follicles were incubated in 10 µM MitoSOX (stock solution: 5 mM in DMSO), 1 µM MitoTracker Deep Red (stock solution: 1 mM in DMSO) and 6 nM Hoechst 33,342 (Thermo Fisher R37605, USA) in MEM plus Glutamax (Gibco, Invitrogen, Belgium) enriched with 10% HIFBS (Thermo Fisher Scientific, USA) for 30 min at 37 °C. They were then fixed in 4% formaldehyde for 20 min at 4 °C. Fixed follicles were collected in channels of a µ-slide VI flat (Ibidi 80,626, Wisconsin, USA), filled with 30 µl PBS and kept in the dark at 4 °C until evaluation.

Each follicle was imaged using a Zeiss LSM 800 confocal microscope at its largest diameter with a 40 × Plan-Apochromat oil immersion objective. Acquisition parameters were kept constant for all experiments. MitoTracker Deep Red, MitoSOX and Hoechst 33,342 were respectively excited with 640-, 561- and 405-nm lasers. For quantitative evaluation, image analysis was performed using ImageJ software. A detection threshold was determined for each marker. Cytoplasmic areas (obtained after nuclei exclusion) stained with each dye were quantified out of total follicle area and expressed as a percentage.

2. Mitochondrial mass evaluation in histological sections

Three non-consecutive sections from each sample were used for immunolabeling of TOMM20, a peptide receptor located on the surface of the outer mitochondrial membrane, as previously reported in the literature [20]. Briefly, after deparaffinization and rehydration, sections were treated to block endogenous peroxidase activity by incubation in 3% hydrogen peroxide (in water) for 30 min and to bind non-specific antibodies by incubation in goat serum for another 30 min. This was followed by overnight incubation at 4 °C with primary antibody (rabbit anti-human TOMM20 (dilution 1:500, PAS-52843, Invitrogen)) and, after subsequent washing, a further 60 min at room temperature with EnVision anti-rabbit secondary antibody (Dako K4003, North Carolina, USA). Diaminobenzidine (DAB Cector 4100, Dako, NC, USA) was used as a chromogenic peroxide substrate and nuclei were counterstained with hematoxylin. Slides were mounted using a Sakura TissueTek coverslipper. Negative controls were in line with current guidelines, using rabbit-specific polyclonal antibody FLEX (ready to use, IS600, Dako, NC, USA) to substitute the primary antibody.

Stained slides were digitized using the Pannoramic P250 Flash III scanner (3DHISTECH, Hungary) at 40 × magnification and visualized with Caseviewer software (v2.3). Images of ovarian tissue areas containing follicles (oocytes, GC layer or entire follicles) were captured with CaseViewer at 40 × magnification and analyzed by Fiji v1.52 (NIH, USA) as previously described [27]. Briefly, PFs were digitally isolated from adjacent stroma by selecting a region of interest (ROI). After determining a threshold for TOMM20 staining, immunolabeled areas and total follicle area were calculated in square micrometers and expressed as a percentage of TOMM20-stained area out of total area per ROI.

Telomere length assessment in ovarian tissue

Formalin-fixed paraffin-embedded 5-µm-thick sections of ovarian tissue were placed on SuperFrost white slides (Fisher Scientific, France) and used to detect telomeres following an established protocol [28]. They were deparaffinized using three consecutive baths in Histosafe for 10 min each, rehydrated through a graded ethanol series at 100%, 95%, 70% and 30% for 3 min each, before being washed in PBS and heated in a microwave at 450 watts for 10 min in citrate buffer (10 mM sodium citrate, 0.1% Tween-20, pH 6). The slides were then cooled down, washed in PBS again and incubated in permeabilization buffer (20 mM Tris–HCl pH8, 50 mM NaCl, 3 mM MgCl2, 300 mM sucrose, 0.5% triton x-100) for 1 h at 37 °C. They were treated with 100 µg/ml RNase A (Qiagen, Germany) diluted in 10% UltraPure 20 × SSC (Thermo Fisher, USA) for 1 h at 37 °C, serially hydrated through a graded ethanol series at 70%, 85% and 100% for 2 min each, then air-dried and overlaid with hybridization solution containing a 160 nM G-richtelomeric LNA probe (Qiagen, Germany), 50% deionized formamide, UltraPure 2 × SSC (Thermo Fisher, USA) and 1 × blocking reagent (Roche Custom Biotech, Germany). The slides were subsequently incubated at 83 °C for 3 min with a coverslip. After 2 h of incubation at room temperature in the dark, the

unbound probe was washed off as follows: twice for 15 min in 50% deionized formamide, UltraPure 2 × SSC (Thermo Fisher, USA), 20 mM Tris–HCl pH 7.4, and twice for 10 min in 150 mM NaCl, 0.05% Tween-20 and 50 mM Tris–HCl pH 7.4. The slides were serially dehydrated again and fixed in 4% formol for 10 min. Nuclei were then stained with Hoechst 33,342 (1:500, Thermo Fisher, USA) and mounted using aqueous mounting medium (Enzo, NY, USA).

Images were acquired with the Zeiss LSM 800 at 63 × objective in oil immersion as a Z-stack, with microscope adjustments kept constant for all experiments. The LNA G-rich probe for telomeres was detected at a wavelength of 568 nm, while Hoechst 33,342 was detected at 405 nm. Quantitative analysis was conducted using ImageJ software. Mean intensity staining of telomere dyes was quantified in each of the following compartments: GCs in PFs, oocytes in PFs, GCs in GFs, oocytes in GFs and stromal cells selected from cortical areas surrounding analyzed follicles.

Telomerase expression by ddPCR

Preantral follicles were isolated from frozen-thawed ovarian cortical strips by mechanical and enzymatic digestion, as described above, before being sorted into two populations according to size (under and over 50 µm) for each patient. Pools of isolated follicles were then stored in RLT lysis buffer at − 80 °C until use. Total ribonucleic acid (RNA) was obtained by RNA extraction with the RNeasy Plus micro kit (Qiagen, Germany) according to the manufacturer's instructions. RNA purity and quantity were assured using the NanoDrop 2000c spectrophotometer (Thermo Scientific). All RNA samples were reverse-transcribed at the same time using the SuperScript IV VILO Master Mix (Invitrogen), while complementary DNA (cDNA) was stored at − 80 °C. FAM-labeled commercial assays were carried out for *hTERT* (Taqman, HS00972650-m1), a catalytic subunit of telomerase, whose expression is restricted to some cells, and *hTERC* (Taqman, Hs03454202_s1), the constitutively expressed RNA subunit of the enzyme.

The QX200 Droplet Digital PCR System (Bio-Rad Laboratories Inc., CA, USA) was used. The reaction mixture contained 11 µl ddPCR™ Supermix for probes (no dUTP), 1-µl assays for the gene of interest or the reference gene, 7 ng cDNA and Tris–EDTA buffer. Twenty-two microliters of this mixture was used and a previously established protocol for ddPCR was applied [27, 29]. Each reaction was run in technical duplicate, with absolute quantification, as this method is preferred for low-input samples where reference gene expression may be variable or unreliable.

The experiment included negative (primary HFF2 foreskin fibroblasts) and positive (U2OS sarcoma cells ectopically overexpressing *hTERT* and *hTERC*) control samples, and no template controls. Droplets were deemed positive or negative by thresholding based on their fluorescence amplitudes. Results were analyzed when reliable amplification was obtained, gene expression levels were consistent between runs in control samples and the number of tested droplets per well was > 10,000.

Results

Ovarian reserve and primordial follicle pool

Follicle density and age showed a negative correlation, as expected (Fig. 1A). Looking at different age groups, mean follicle density was 965.85 (range 49.9–2010.03) in the young-age group (20–26, $n = 7$), 154.56 (range 57.49–546.37) in the mid-age group (27–36, $n = 6$) and 59.83 (range 26.66–178.85) in the advanced-age group (37–46, $n = 8$) ($p < 0.01$) (Fig. 1B). Proportions of PFs out of total follicles also correlated negatively with increasing age, yielding 87.93 ± 12.57 (mean %, ± SD) in the young-age group, 70.5 ± 16.99 in the mid-age group and 59.92 ± 11.55 in the advanced-age group ($p < 0.01$) (Fig. 1C). Atretic follicle rates were not linked to age and showed values of 21.85 ± 9.86 (mean %, ± SD) in the young-age group, 18.66 ± 15.89 in the mid-age group and 19.48 ± 10.83 in the advanced-age group (Fig. 1D).

Mitochondrial mass, function and oxidative stress

Mitochondrial mass marker TOMM20 was stable with increasing age, as similar mean levels were detected between different age groups in analyzed preantral follicle pools, specifically 26.51 ± 11.37 (mean %, ± SD) in the young-age group, 27.12 ± 12.1 in the mid-age group and 26.36 ± 12.13 in the advanced-age group (Fig. 2A–B). When observing TOMM20 expression in follicle compartments, the GC layer was found to have increased the signal significantly more than oocytes with follicle growth (GCs: 16.66 ± 9 vs. 30.19 ± 14.5; oocytes: 23.42 ± 10.23 vs. 27.15 ± 13.5) (Fig. 3C). When considering TOMM20 expression in PFs compared to GFs (Fig. 2D) in all age groups, a significant upturn was detected in mitochondrial mass along with GF stage in young patients (24.94 ± 10.27 vs. 30.37 ± 13.69, $p < 0.01$). An upward trend was also noted in the mid-age group (25.06 ± 11.77 vs. 33.16 ± 18.87), while similar levels were encountered in advanced-age patients (26.21 ± 11.47 vs. 29.55 ± 12.83) (Fig. 2E–F).

Among mitochondrial markers, namely MitoTracker Deep Red and MitoSOX for active mitochondria and ROS generation respectively (Fig. 3A), there were no changes between the different age groups. Active mitochondria numbered 18.49 ± 8.08 (mean %, ± SD) in the young-age group,

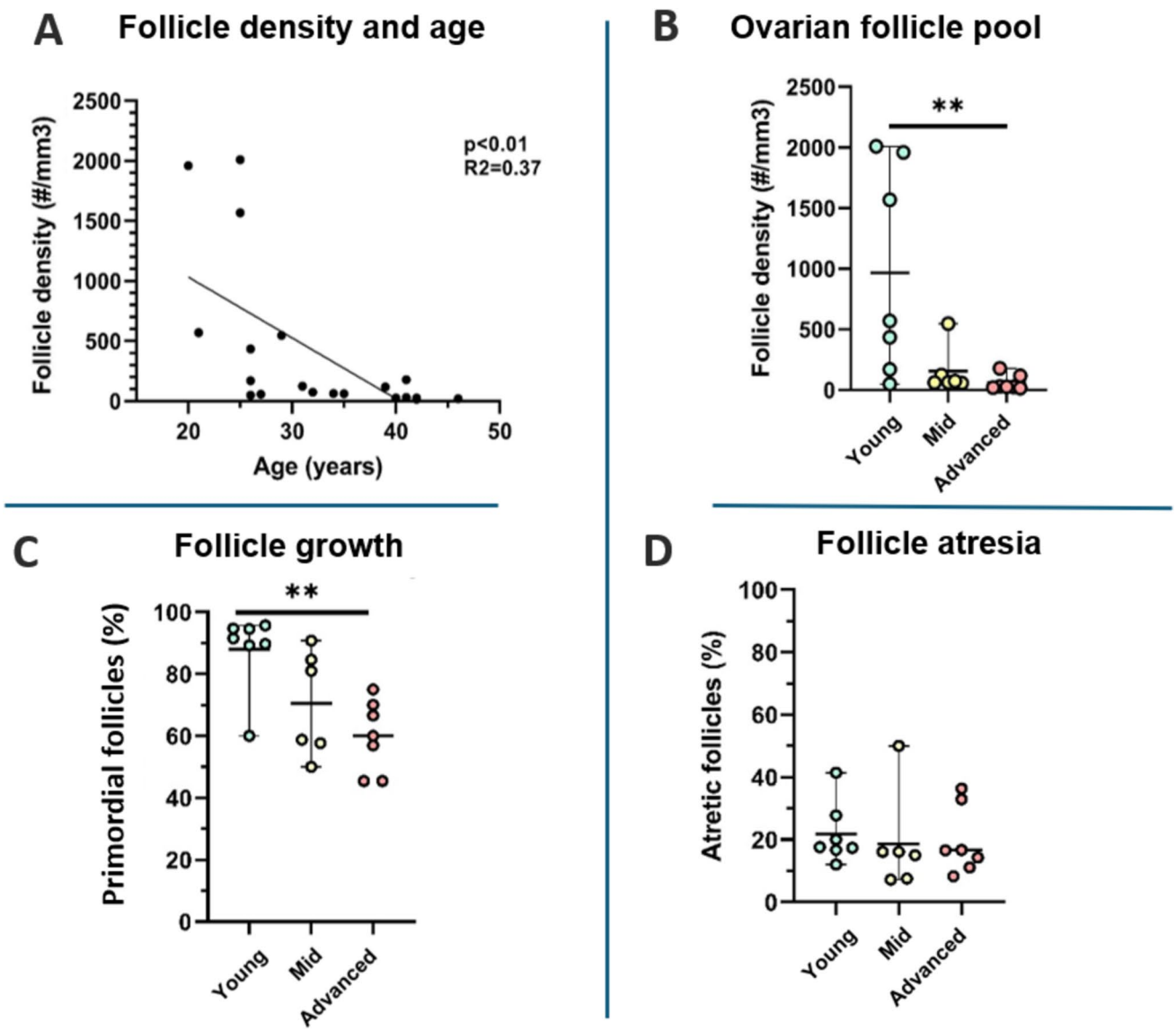

Fig. 1 **A** Linear regression between age and follicle density ($p < 0.01$, $R^2 = 0.37$). **B** Ovarian follicle pool residing in the cortex expressed as total follicle density (#/mm^3) in the three age groups. **C** Proportions of primordial follicles (PFs) in the three age groups. **D** Proportions of atretic follicles in the three age groups

14.49 ± 8.52 in the mid-age group and 18.70 ± 9.38 in the advanced-age group (Fig. 3B), while ROS generation was respectively 11.85 ± 6.71, 16.1 ± 6.44 and 10.46 ± 4.53 (Fig. 3F). When comparing expression in PFs and GFs for each age group, no differences were observed in active mitochondria stained with MitoTracker Deep Red, numbering 20.37 ± 9.82 in PFs and 17.27 ± 8.76 in GFs in the young-age group, 13.47 ± 12.27 in PFs and 14.54 ± 1.5 in GFs in the mid-age group and 19.24 ± 7.91 in PFs and 21.83 ± 15.88 in GFs in the advanced-age group (Fig. 3C–E). On the other hand, ROS generation detected by MitoSOX dropped significantly with follicle growth in the young-age group (14.74 ± 7.84 in PFs versus 9.14 ± 5.45 in GFs, $p < 0.01$), rose with follicle growth in the mid-age group (13.14 ± 6.06 in PFs versus 23.67 ± 7.54 in GFs, $p < 0.05$) and showed inconsistent variations in the advanced-age group (9.66 ± 5.38 in PFs versus 10.53 ± 7.7 in GFs) (Fig. 3G–I). As a marker of functional mitochondria, MitoTracker Deep Red signal quantification did not correlate with age nor TOMM20 levels in isolated follicles (Supplementary Information 2).

Telomere length in peripheral lymphocytes and in ovarian tissue

Telomere length in peripheral lymphocytes of these 20 women ranged between the 1 st and 97.5th percentiles of

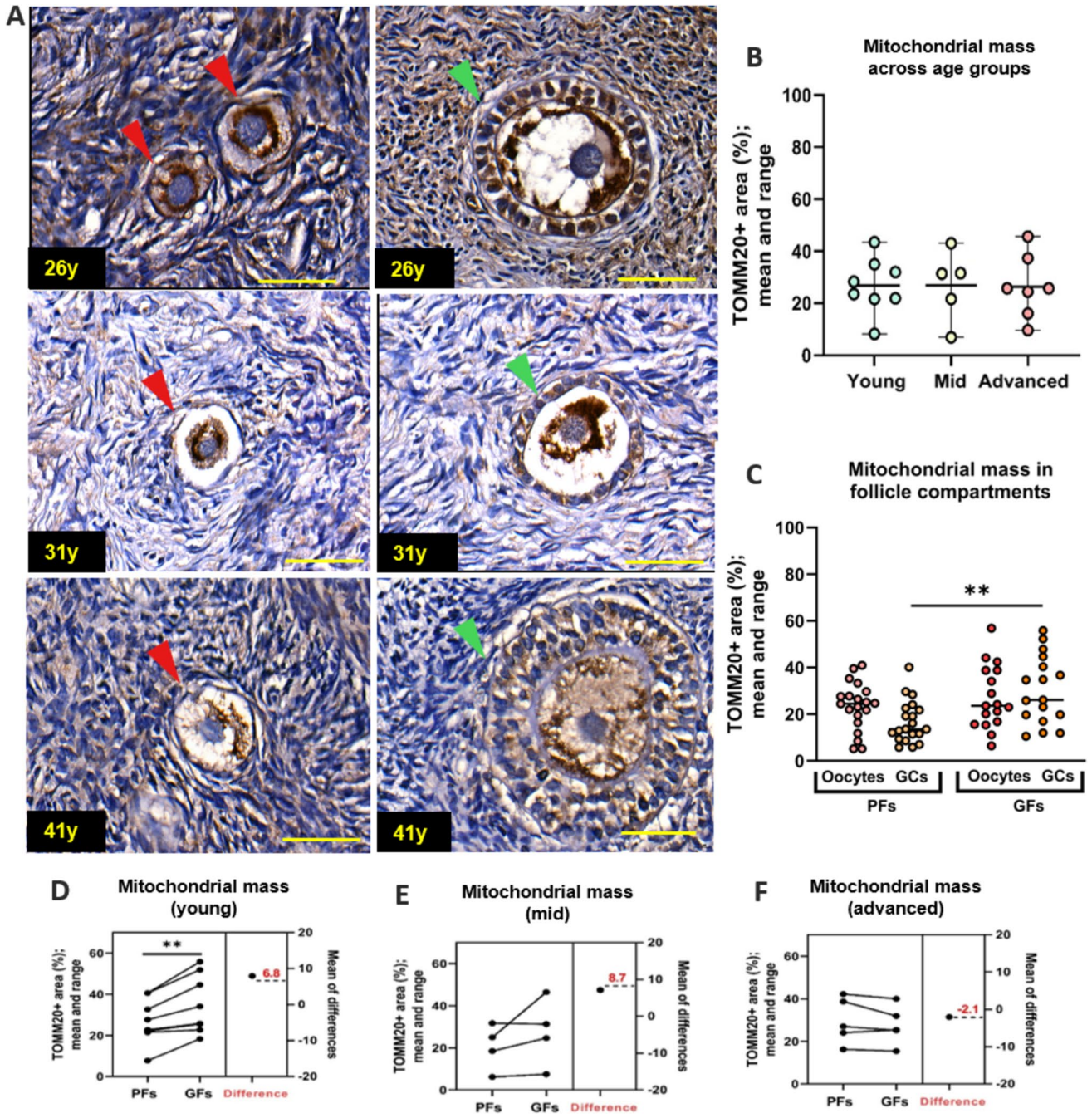

Fig. 2 **A** Representative images of TOMM20 staining in primordial follicles (PFs) (red arrows) and growing follicles (GFs) (green arrows) in human ovarian tissue of three patients aged 26, 31 and 41 years respectively. Scale bar: 50 µm. **B** Proportions of TOMM20-stained area in the preantral follicle pool as a marker of mitochondrial mass in the three age groups. Each dot represents the mean value obtained for follicles detected on 6 sections per sample. **C** Proportions of TOMM20-stained area in oocytes and granulosa cell (GC) layer. **D**, **E**, **F** Paired *t*-test for TOMM20 + area in PFs and GFs in the three age groups. $*p < 0.05$; $**p < 0.001$

a reference cohort from Cliniques Universitaires Saint Luc, indicating no bias in the cohort (Fig. 4A), and showed a tendency to decrease with increasing age (Fig. 4B). Average telomere length was evaluated in each compartment of ovarian tissue, namely the stroma, GCs and oocytes from PFs and GFs, collected from a total of 20 subjects (Fig. 4C).

Comparison of telomere length between age groups did not evidence any significant variation in this parameter with increasing age. In the young-age group, telomere length was 26.64 ± 11.35 in GCs and 27.98 ± 12.69 in oocytes of PFs, 28.57 ± 11.32 in stromal cells and 31.1 ± 11.61 in GC layers of GFs. In the mid-age group,

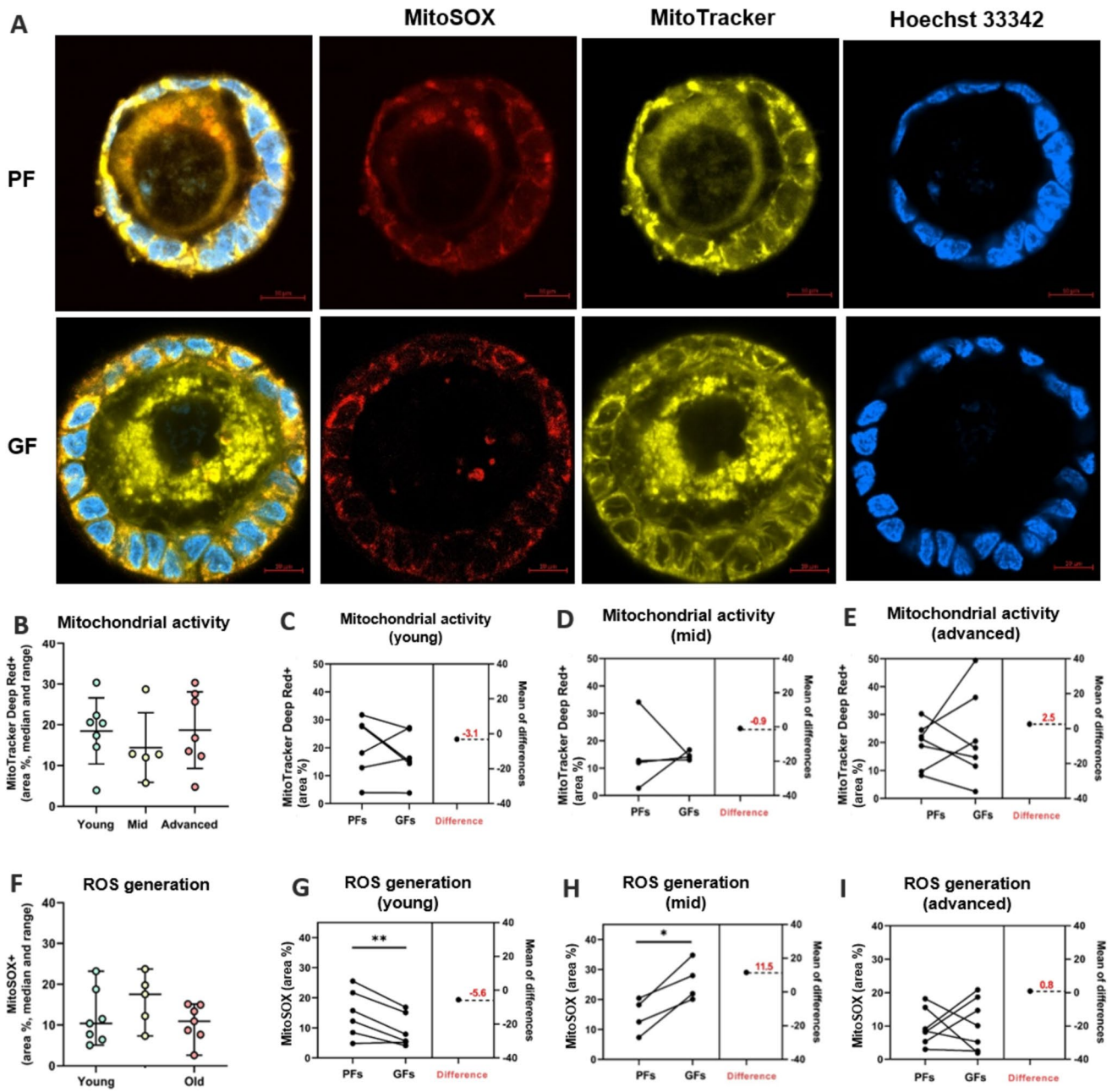

Fig. 3 **A** Representative images of isolated primordial follicles (PFs) and growing follicles (GFs) stained live with MitoSOX and MitoTracker Deep Red, then fixed and analyzed by confocal microscopy (40×). Images were captured in the central plane of the Z-stack acquired for each 3D-stained follicle. For each follicle, the panel shows (from left to right) the merged image, followed by individual channels for MitoSOX (red), MitoTracker Deep Red (yellow) and Hoechst 33,342 (blue). Scale bar: 10 µm. **B** Proportions of average MitoTracker Deep Red-stained area in isolated preantral follicles as a marker of mitochondrial activity in the three age groups. **C**, **D**, **E** Paired *t*-test for MitoTracker Deep Red-stained area in PFs and GFs in the three age groups. **F** Proportions of average MitoSOX-positive area in isolated preantral follicles as a marker of mitochondrial ROS generation in the three age groups. **G**, **H**, **I** Paired *t*-test for MitoSOX + area in PFs and GFs in the three age groups. $*p < 0.05$; $**p < 0.001$

values were 23.27 ± 8.85 and 21.11 ± 11.1 in GCs and oocytes of PFs, 24.81 in stromal cells and 27.76 ± 9.6 in GC layers of GFs. In the advanced-age group, telomere length was 33.5 ± 20.01 and 37.04 ± 23.66 in GCs and oocytes of PFs, 36.77 ± 18.19 in stromal cells and 40.84 ± 14.30 in GC layers of GFs (Fig. 4D).

Analysis of telomere dynamics in different tissue compartments for each patient group was also conducted. Similar

telomere length was detected between GCs and oocytes in PFs in all age range groups (Fig. 4E–G). Comparisons between GCs and oocytes in GFs were not made, as numbers of oocytes visible by immunofluorescence-FISH for this follicle stage were not sufficient. Significantly longer telomeres were spotted in GCs of GFs than in PFs at all ages (young: $p < 0.01$; mid: $p < 0.05$; advanced: $p < 0.05$) (Fig. 4H–J). Significantly longer telomeres were found in stromal cells compared to GCs of PFs in younger patients ($p < 0.05$), while in the mid-age and advanced-age groups, this difference was not significant (Fig. 4K–M). No correlation was established between these parameters and age, follicle density or telomere length within ovarian tissue (Supplementary Table 2).

Telomerase expression

Expression of *hTERC* was detected in both positive and negative controls, while *hTERT* expression was evidenced only in positive controls (Fig. 5A). In PFs and GFs, *hTERC* and *hTERT* were not always identified, and no significant difference was observed between them (Fig. 5B).

Discussion

Age-related decline in female fertility leads to a reduced probability of conception every month and increased risk of implantation failure or early fetal loss. Infertility rates, defined as a delay in conception after more than 1 year of attempts, range from 6% in young women (15–24 years) to over 30% in women of late reproductive age (35–44 years) [29]. This age-associated decline in fertility over time is characterized by quantitative and qualitative alterations to the ovarian reserve.

In terms of quantitative modifications, studies based on large numbers of histological samples have shown that the ovarian follicle pool diminishes with age, resulting in a loss of about 85% of follicles over a woman's lifespan [30, 31]. Our findings are fully in line with the literature, confirming a drop in the ovarian follicle pool by the age of 37–38 years. Regarding qualitative alterations, the literature focuses on a number of key cell functions at later stages of folliculogenesis, including energy supply and genetic stability, involved in the decline of oocyte fertilization, embryo development and further implantation [32–34].

Our investigations revealed that mitochondrial mass, assessed by TOMM20 expression, remains relatively stable across age groups in PFs, with no significant age-related downturn. However, there was a notable increase in mitochondrial mass, especially in the GC layer, probably due to mitochondrial biogenesis during initial follicle growth in younger patients, a trend that was less pronounced or absent in older subjects. These findings suggest that mitochondrial biogenesis dynamics change with age during early folliculogenesis, in line with the mitochondrial bottleneck theory, whereby PFs maintain a minimal and relatively mutation-free mitochondrial pool that must expand upon activation and growth [13, 19]. Our experimental model does not allow us to determine whether this age-related difference reflects enhanced biogenesis in younger individuals or impaired capacity in older ones. However, the known decline in mtDNA copy number and stability with advancing age, also key parameters of mitochondrial function and biogenesis may support the hypothesis of reduced mitochondrial biogenesis in the aging ovary [35].

Active mitochondria, as detected by MitoTracker Deep Red, did not reveal any significant age-dependent variations, nor was there any correlation with TOMM20 levels. This may seem to contradict previous studies showing impaired mitochondrial function in oocytes from women of late reproductive age [15, 16]. It is possible that the mitochondrial impairment described in the recent literature as occurring at later stages of oocyte maturation is not yet apparent at earlier stages of folliculogenesis, which were the main focus of our study. Nevertheless, ROS generation marked by MitoSOX and representing one of the signs of mitochondrial dysfunction in cells [36] exhibited complex patterns, with a significant drop in ROS values during follicle growth in young patients, but increased levels with follicle growth in the mid-age group. In our study, mitochondria from younger subjects appeared to function more effectively, as indicated by reduced production of ROS as byproducts of the respiratory chain. While this suggests possible age-related impairment of mitochondria, we acknowledge that ROS measurements alone are not sufficient to draw conclusions about oxidative damage or antioxidant capacity, which were not assessed in the present study. Whether or not this increase in ROS in older subjects is counterbalanced by a complementary rise in antioxidant defenses, it may still reflect an underlying vulnerability in mitochondrial function. Notably, this alteration arises at a critical stage when mitochondrial biogenesis and activity should intensify to support early follicle growth, potentially contributing to impaired follicle and oocyte maturation with advancing age [37].

Genetic stability, particularly telomere length regulation, is essential for safe DNA replication in somatic cells. While telomere length is typically linked to aging [8], we did not find it useful among reproductive-age subjects (20–46 years). We observed no correlation between telomere length in peripheral leukocytes and ovarian compartments. This may be due to wide interindividual variability in leukocyte telomere length during the reproductive years, which could hide weak correlations unless studied in large cohorts. Alternatively, telomere dynamics may be regulated by tissue-specific mechanisms, limiting the usefulness of

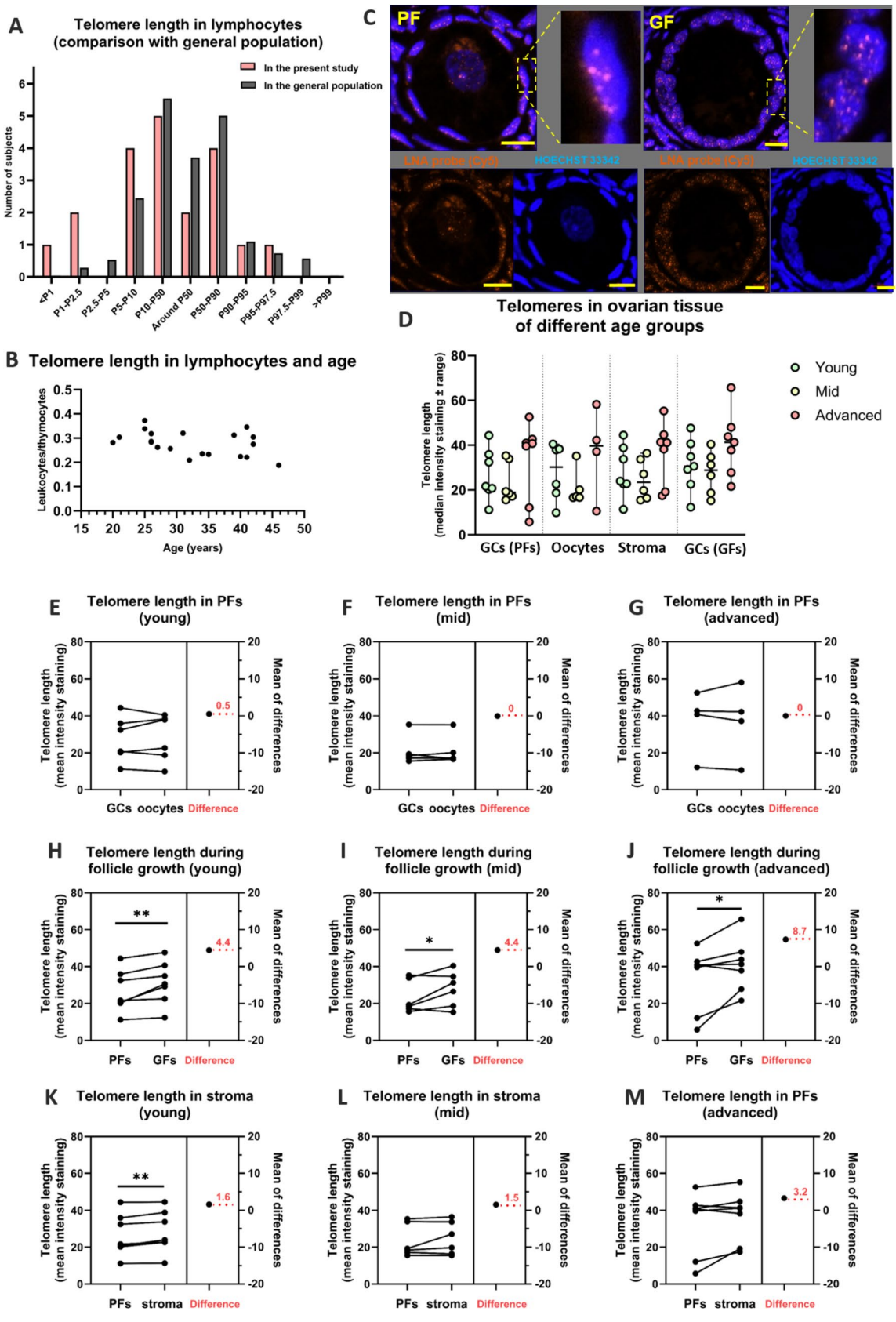
A
Telomere length in lymphocytes (comparison with general population)
In the present study
In the general population
Number of subjects
<P1
P1-P2.5
P2.5-P5
P5-P10
P10-P50
Around P50
P50-P90
P90-P95
P95-P97.5
>P99
B Telomere length in lymphocytes and age
Leukocytes/thymocytes
Age (years)
C
PF
GF
LNA probe (Cy5)
HOECHST 33342
D
Telomeres in ovarian tissue of different age groups
Telomere length (median intensity staining ± range)
GCs (PFs)
Oocytes
Stroma
GCs (GFs)
Young
Mid
Advanced
E Telomere length in PFs (young)
F Telomere length in PFs (mid)
G Telomere length in PFs (advanced)
H Telomere length during follicle growth (young)
I Telomere length during follicle growth (mid)
J Telomere length during follicle growth (advanced)
K Telomere length in stroma (young)
L Telomere length in stroma (mid)
M Telomere length in PFs (advanced)
Telomere length (mean intensity staining)
Mean of differences
GCs oocytes Difference
PFs GFs Difference
PFs stroma Difference

◂**Fig. 4** **A** Distribution of telomere length in the 20 subjects included in the study compared to a reference population at Cliniques Universitaires Saint Luc. **B** Correlation between telomere length in lymphocytes and age. **C** Representative image of FISH analysis showing telomeres in a primordial follicle (PF) and a growing follicle (GF). FISH was performed on tissue sections, and telomere signals were evaluated in different cell compartments, including granulosa cells (GCs) from both PFs and GFs, as shown in the examples. Images were acquired by confocal microscopy at 63×. In the lower panel, individual fluorescence channels are shown for each follicle: red for the telomere-specific LNA probe (Cy5) and blue for Hoechst 33,342. Scale bar: 10 µm. **D** Mean telomere length in GCs and oocytes of PFs, stromal cells and GCs of GFs in the three age groups. **E**, **F**, **G** Paired *t*-test of mean telomere length in GCs and oocytes of PFs in the three age groups. **H**, **I**, **J** Paired *t*-test of mean telomere length in GCs of PFs and GCs of GFs in the three age groups. **K**, **L**, **M** Paired *t*-test of mean telomere length in GCs of PFs and stromal cells in the three age groups. $*p < 0.05$; $**p < 0.001$

leukocyte telomere length as a surrogate marker of ovarian aging [7, 8, 38].

When analyzing telomere length in ovarian tissue across different cell types, namely GCs, oocytes and stromal cells, we made several important observations. In all age groups, GCs from GFs exhibited significantly longer telomeres than those in PFs, suggesting that the intrinsic ability to maintain or elongate telomeres during early follicle growth is preserved throughout the reproductive lifespan. This telomere elongation in GCs is likely essential to sustain their proliferative capacity during maturation [39, 40]. By contrast, telomere dynamics in surrounding stromal cells appeared to be age-dependent, showing possible loss of regulatory capacity with increasing age. This could reflect extrinsic changes in the ovarian microenvironment rather than intrinsic deficits within follicular cells themselves. Indeed, it is well established that the ovarian stroma undergoes structural and functional remodeling with advancing age, including altered collagen deposition, immune dysregulation and a shift toward a more inflammatory and pro-oxidative milieu [41]. Telomeres, being guanosine-rich, are particularly susceptible to oxidative stress. As ROS accumulate with age, they may exacerbate telomere attrition in stromal cells, potentially contributing to premature cell cycle arrest and impaired support of follicle development [42, 43]. These findings suggest that telomere regulation within follicles is largely preserved, while age-related changes in the surrounding stroma may impair overall follicle function. This remodeling may represent a physiological process that becomes disrupted in women with a diminished ovarian reserve. Previous studies have indeed shown that telomeres are shorter and richer in DNA aberrations in cumulus GCs in women with poor fertility due to advanced age or a decreased ovarian stockpile [8, 11, 12]. Like other epigenetic markers, such as DNA methylation, telomere length in cumulus GCs correlates with a 'younger' biological age when analyzed through epigenetic clocks [7, 38]. Telomere remodeling, particularly elongation, primarily occurs via telomerase, an enzyme highly conserved across species [44]. Telomerase activity has been detected in GCs of antral and cumulus layers in pigs [45, 46] and bovines [47, 48], yielding longer telomeres, but not in PFs [47]. The present study is the first to show telomerase expression in human PFs and early GFs. We were not able to determine whether telomerase activity occurred in GCs, oocytes or both. Given the oocyte/GC ratio, approximately 1:100 in PFs and up to 1:1000 in secondary follicles, we can infer that telomerase gene expression originated from GCs, which may well need telomerase activation for safe DNA replication during their further proliferation [49]. It is known that adult germ cells lack telomerase activity, unlike fetal germ cells [50], which might explain why oocytes do not have longer telomeres than their surrounding GCs. This suggests that human oocytes do not maintain telomere length for long-term survival and proper meiosis, contributing to their diminishing quality with age [40].

Strengths and limitations

One of the strengths of this study is the use of human ovarian tissue samples across a broad age range, allowing for a comprehensive analysis of mitochondrial and telomere dynamics at early follicle stages. One of its drawbacks is the application of strict selection criteria for women with no history of infertility, which could have led to potential bias in older patients, having recruited women of proven and/or high fertility compared to other age ranges.

This study was exploratory in nature and not based on prior power analysis. Its primary objective was to characterize the behavior of mitochondrial and telomeric markers during early follicle growth in an underexplored, non-stimulated human ovarian context. The histological techniques and live-cell dyes used, while appropriate for spatially resolving mitochondrial markers within each follicle stage, provide only indirect proof of mitochondrial dynamics and lack the capacity to capture functional processes like ATP production and oxygen consumption. Despite these limitations, several significant trends were observed that may inform new hypotheses and future targeted studies. More specifically, mitochondria and telomere regulation were found to occur differently in younger subjects than in other subjects. This means that follicle growth disruption due to age-related events like lower energy supply, oxidative stress and unsafe DNA replication could occur already at preantral follicle stages in women with age-related reproductive issues. Future challenges in reproductive medicine will involve the development of therapeutic strategies to address cell dysfunction like ROS accumulation during early follicle growth, which lasts 4–6 months before the FSH-dependent phase and for which there is no available treatment as yet.

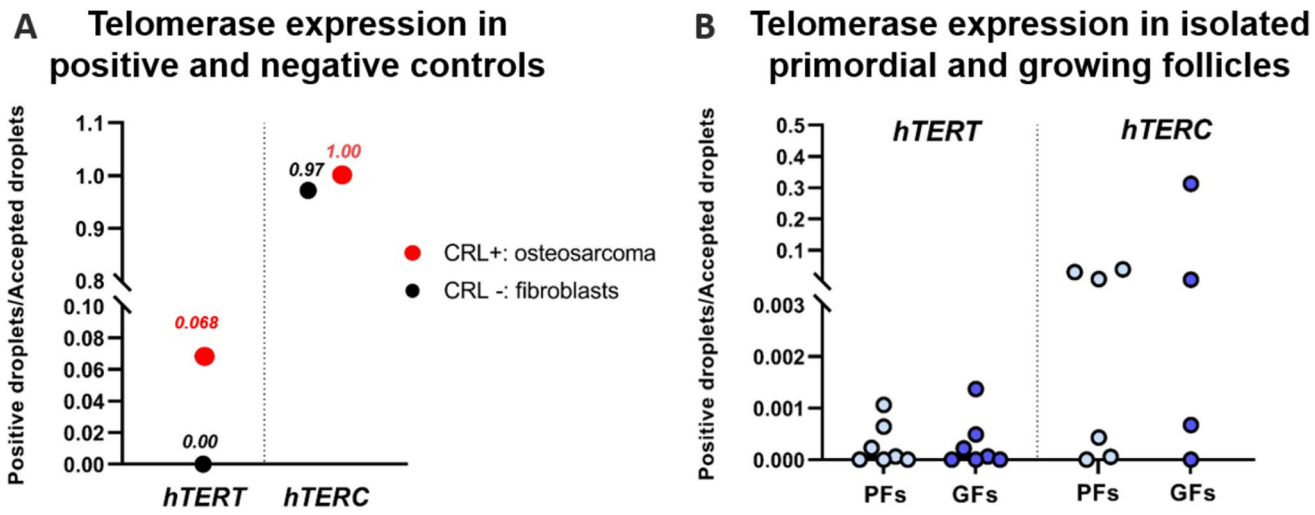

Fig. 5 **A** *hTERT* and *hTERC* expression in positive and negative controls. **B** *hTERT* and *hTERC* expression in primordial follicles (PFs, < 50 µm) and growing follicles (GFs, > 50 µm)

Conclusions

This study provides new insights into mitochondrial and telomere dynamics during early folliculogenesis in human ovarian tissue across the reproductive age range. Specifically, we observed an age-dependent increase in mitochondrial mass accompanied by lower levels of ROS generation in younger individuals, while telomere lengthening during early follicle growth occurred consistently across all age groups. By contrast, telomere regulation in stromal cells appeared to be increasingly altered with age. By capturing these changes at defined early stages of folliculogenesis, the study helps pinpoint when age-related alterations begin to emerge in the timeline of follicle development. These findings enhance our understanding of the cellular mechanisms involved in ovarian aging, and may inform future studies investigating how their disruption is linked to a diminished ovarian reserve and impaired oocyte quality.

Supplementary information The online version contains supplementary material available at https://doi.org/10.1007/s10815-025-03721-0.

Acknowledgements The authors thank Prof, Anabelle Decottignies for her assistance with telomere length measurements, Mira Hryniuk, B.A., for reviewing the English language of the article and Olivier van Kerk, Manon Mahieu and Joachim Ravau for their technical assistance.

Author contributions LC: design, experimental execution, analysis, manuscript writing; MZ: experimental execution and analysis; LH: experimental execution; CB: analysis; MAV: experimental execution and analysis; ML: sample allocation procedures; JD: manuscript review; MMD: experimental design and manuscript review.

Funding This study was supported by grants from the Fonds National de la Recherche Scientifique de Belgique (FNRS-PDR T.0077.14, FNRS-CDR J.0063.20, grant 5/4/150/5 awarded to MMD and Scientific Collaborator Mandate to LC) and the China Scholarship Council (CSCNO.202308530003 awarded to MZ).

Data availability Data underlying this article will be made available by the corresponding author upon reasonable request.

Declarations

Ethics approval Use of human ovarian tissue and blood samples was approved by the Institutional Review Board of the Université Catholique de Louvain (Reference: 2012/23MAR/125).

Competing interests The authors declare no competing interests.

References

1. Dolmans MM, Donnez J. Fertility preservation in women for medical and social reasons: oocytes vs ovarian tissue. Best Pract Res Clin Obstet Gynaecol. 2021;70:63–80. https://doi.org/10.1016/j.bpobgyn.2020.06.011.
2. Wolfe JD, Thomeer MB, Reczek R. Age at first birth and women's midlife health: cohort and race differences across the 20th century. Soc Sci Med. 2023;331:116097. https://doi.org/10.1016/j.socscimed.2023.116097.
3. Mishra SR, Chung HF, Waller M, Mishra GD. Duration of estrogen exposure during reproductive years, age at menarche and age at menopause, and risk of cardiovascular disease events, all-cause and cardiovascular mortality: a systematic review and meta-analysis. BJOG. 2021Apr;128(5):809–21. https://doi.org/10.1111/1471-0528.16524.
4. Garg A, Seli E. Leukocyte telomere length and DNA methylome as biomarkers of ovarian reserve and embryo aneuploidy: the intricate relationship between somatic and reproductive aging. Fertil Steril. 2024;121(1):26–33. https://doi.org/10.1016/j.fertnstert.2023.11.011.
5. Ferreira AF, Soares M, Almeida-Santos T, Ramalho-Santos J, Sousa AP. Aging and oocyte competence: a molecular cell

perspective. WIREs Mech Dis. 2023;15(5):e1613. https://doi.org/10.1002/wsbm.1613.
6. Alberico HC, Woods DC. Role of granulosa cells in the aging ovarian landscape: a focus on mitochondrial and metabolic function. Front Physiol. 2022;12:800739. https://doi.org/10.3389/fphys.2021.800739.
7. Khan SA, Reed L, Schoolcraft WB, Yuan Y, Krisher RL. Control of mitochondrial integrity influences oocyte quality during reproductive aging. Mol Hum Reprod. 2023;29(9):gaad028. https://doi.org/10.1093/molehr/gaad028.
8. Olsen KW, Castillo-Fernandez J, Zedeler A, Freiesleben NC, Bungum M, Chan AC, et al. A distinctive epigenetic ageing profile in human granulosa cells. Hum Reprod. 2020;35(6):1332–45. https://doi.org/10.1093/humrep/deaa071.
9. Lara-Molina EE, Franasiak JM, Marin D, Tao X, Díaz-Gimeno P, Florensa M, et al. Cumulus cells have longer telomeres than leukocytes in reproductive-age women. Fertil Steril. 2020;113(1):217–23. https://doi.org/10.1016/j.fertnstert.2019.08.089.
10. Sethuram R, Bazzi AA, Salih SM, Puscheck EE. Peripheral lymphocyte telomere dysfunction: a valid surrogate marker for female fertility? Fertil Steril. 2021;115(1):85–6. https://doi.org/10.1016/j.fertnstert.2020.10.063.
11. Morin SJ, Tao X, Marin D, Zhan Y, Landis J, Bedard J, et al. DNA methylation-based age prediction and telomere length in white blood cells and cumulus cells of infertile women with normal or poor response to ovarian stimulation. Aging (Albany NY). 2018;10(12):3761–73. https://doi.org/10.18632/aging.101670.
12. M'kacher R, Colicchio B, Marquet V, Borie C, Najar W, Hempel WM, et al. Telomere aberrations, including telomere loss, doublets, and extreme shortening, are increased in patients with infertility. Fertil Steril. 2021;115(1):164–73. https://doi.org/10.1016/j.fertnstert.2020.07.005.
13. May-Panloup P, Boucret L, Chao de la Barca JM, Desquiret-Dumas V, Ferré-L'Hotellier V, Morinière C, Descamps P, Procaccio V, Reynier P. Ovarian ageing: the role of mitochondria in oocytes and follicles. Hum Reprod Update. 2016 Nov;22(6):725–743. https://doi.org/10.1093/humupd/dmw028.
14. Cacciottola L, Donnez J, Dolmans MM. Oxidative stress, mitochondria, and infertility: is the relationship fully established? Fertil Steril. 2021;116(2):306–8. https://doi.org/10.1016/j.fertnstert.2021.04.026.
15. Boucret L, Chao de la Barca JM, Morinière C, Desquiret V, Ferré-L' Hôtellier V, Descamps P, Marcaillou C, Reynier P, Procaccio V, May-Panloup P. Relationship between diminished ovarian reserve and mitochondrial biogenesis in cumulus cells. Hum Reprod. 2015 Jul;30(7):1653–64. https://doi.org/10.1093/humrep/dev114.
16. Jiang Z, Shi C, Han H, Wang Y, Liang R, Chen X, et al. Mitochondria-related changes and metabolic dysfunction in low prognosis patients under the POSEIDON classification. Hum Reprod. 2021;36(11):2904–15. https://doi.org/10.1093/humrep/deab203.
17. Smits MAJ, Schomakers BV, van Weeghel M, Wever EJM, Wüst RCI, Dijk F, et al. Human ovarian aging is characterized by oxidative damage and mitochondrial dysfunction. Hum Reprod. 2023;2(11):2208–20. https://doi.org/10.1093/humrep/dead177.
18. Johnston IG, Burgstaller JP, Havlicek V, Kolbe T, Rülicke T, Brem G, et al. Stochastic modelling, Bayesian inference, and new in vivo measurements elucidate the debated mtDNA bottleneck mechanism. Elife. 2015;4:e07464. https://doi.org/10.7554/eLife.07464.
19. Babayev E, Wang T, Szigeti-Buck K, Lowther K, Taylor HS, Horvath T, et al. Reproductive aging is associated with changes in oocyte mitochondrial dynamics, function, and mtDNA quantity. Maturitas. 2016;93:121–30. https://doi.org/10.1016/j.maturitas.2016.06.015.
20. Masciangelo R, Chiti MC, Camboni A, Amorim CA, Donnez J, Dolmans MM. Mitochondrial content, activity, and morphology in prepubertal and adult human ovaries. J Assist Reprod Genet. 2021;38(10):2581–90. https://doi.org/10.1007/s10815-021-02282-2.
21. Moustakli E, Zikopoulos A, Sakaloglou P, Bouba I, Sofikitis N, Georgiou I. Functional association between telomeres, oxidation and mitochondria. Front Reprod Health. 2023;5:1107215. https://doi.org/10.3389/frph.2023.1107215.
22. Assalve G, Lunetti P, Rocca MS, Cosci I, Di Nisio A, Ferlin A, et al. Exploring the link between telomeres and mitochondria: mechanisms and implications in different cell types. Int J Mol Sci. 2025;26(3):993. https://doi.org/10.3390/ijms26030993.
23. Ju W, et al. Mechanisms of mitochondrial dysfunction in ovarian aging and potential interventions. Front Endocrinol (Lausanne). 2024Apr;17(15):1361289.
24. Baerlocher GM, Vulto I, de Jong G, Lansdorp PM. Flow cytometry and FISH to measure the average length of telomeres (flow FISH). Nat Protoc. 2006;1(5):2365–76. https://doi.org/10.1038/nprot.2006.263.
25. Chiti MC, Dolmans MM, Hobeika M, Cernogoraz A, Donnez J, Amorim CA. A modified and tailored human follicle isolation procedure improves follicle recovery and survival. J Ovarian Res. 2017;10(1):71. https://doi.org/10.1186/s13048-017-0366-8.
26. Gougeon A, Chainy GB. Morphometric studies of small follicles in ovaries of women at different ages. J Reprod Fertil. 1987;81(2):433–42. https://doi.org/10.1530/jrf.0.0810433.
27. Hossay C, Tramacere F, Cacciottola L, Camboni A, Squifflet JL, Donnez J, et al. Follicle outcomes in human ovarian tissue: effect of freezing, culture, and grafting. Fertil Steril. 2023;119(1):135–45. https://doi.org/10.1016/j.fertnstert.2022.09.360.
28. Barretta M, Cacciottola L, Hossay C, Donnez J. Impact of human ovarian tissue manipulation on follicles: evidence of a potential first wave of follicle activation during fertility preservation procedures. J Assist Reprod Genet. 2023;40(12):2769–76. https://doi.org/10.1007/s10815-023-02930-9.
29. Nguyen TYT, Cacciottola L, Camboni A, Ravau J, De Vos M, Demeestere I, et al. Ovarian tissue cryopreservation and transplantation in patients with central nervous system tumours. Hum Reprod. 2021;36(5):1296–309. https://doi.org/10.1093/humrep/deaa353.
30. te Velde ER, Pearson PL. The variability of female reproductive ageing. Hum Reprod Update. 2002 Mar-Apr;8(2):141–54. https://doi.org/10.1093/humupd/8.2.141.
31. Wallace WH, Kelsey TW. Human ovarian reserve from conception to the menopause. PLoS ONE. 2010;5(1):e8772. https://doi.org/10.1371/journal.pone.0008772.
32. Ata B, Seyhan A, Seli E. Diminished ovarian reserve versus ovarian aging: overlaps and differences. Curr Opin Obstet Gynecol. 2019;31(3):139–47. https://doi.org/10.1097/GCO.0000000000000536.
33. Charalambous C, Webster A, Schuh M. Aneuploidy in mammalian oocytes and the impact of maternal ageing. Nat Rev Mol Cell Biol. 2023;24(1):27–44. https://doi.org/10.1038/s41580-022-00517-3.
34. Mihalas BP, Marston AL, Wu LE. Reproductive ageing: metabolic contribution to age-related chromosome missegregation in mammalian oocytes. Reproduction. 2024;168(2):e230510. https://doi.org/10.1530/REP-23-0510.
35. Sadeesh EM, Singla N, Lahamge MS, Kumari S, Ampadi AN, Anuj M. Tissue heterogeneity of mitochondrial activity, biogenesis and mitochondrial protein gene expression in buffalo. Mol Biol Rep. 2023;50(6):5255–66. https://doi.org/10.1007/s11033-023-08416-2.
36. Mukhopadhyay P, Rajesh M, Haskó G, Hawkins BJ, Madesh M, Pacher P. Simultaneous detection of apoptosis and mitochondrial superoxide production in live cells by flow cytometry and confocal microscopy. Nat Protoc. 2007;2(9):2295–301. https://doi.org/10.1038/nprot.2007.327.

37. Martin JH, Nixon B, Cafe SL, Aitken RJ, Bromfield EG, Lord T. Oxidative stress and reproductive function: oxidative stress and in vitro ageing of the post-ovulatory oocyte: an update on recent advances in the field. Reproduction. 2022Oct 26;164(6):F109–24.
38. Hood RB, Everson TM, Ford JB, Hauser R, Knight A, Smith AK, et al. Epigenetic age acceleration in follicular fluid and markers of ovarian response among women undergoing IVF. Hum Reprod. 2024;39(9):2003–9. https://doi.org/10.1093/humrep/deae136.
39. Bodnar AG, Ouellette M, Frolkis M, Holt SE, Chiu CP, Morin GB, et al. Extension of life-span by introduction of telomerase into normal human cells. Science. 1998;16(5349):349–52. https://doi.org/10.1126/science.279.5349.349.
40. Ozturk S, Sozen B, Demir N. Telomere length and telomerase activity during oocyte maturation and early embryo development in mammalian species. Mol Hum Reprod. 2014;20(1):15–30. https://doi.org/10.1093/molehr/gat055.
41. Cacciottola L, Camboni A, Dolmans MM. Immune system regulation of physiological and pathological aspects of the ovarian follicle pool throughout the female reproductive lifespan. Hum Reprod. 2025;1(1):12–22. https://doi.org/10.1093/humrep/deae254.
42. Keefe DL, Marquard K, Liu L. The telomere theory of reproductive senescence in women. Curr Opin Obstet Gynecol. 2006;18(3):280–5. https://doi.org/10.1097/01.gco.0000193019.05686.49.
43. Keefe DL, Liu L, Marquard K. Telomeres and aging-related meiotic dysfunction in women. Cell Mol Life Sci. 2007Jan;64(2):139–43. https://doi.org/10.1007/s00018-006-6466-z.
44. Greider CW, Blackburn EH. Identification of a specific telomere terminal transferase activity in *Tetrahymena* extracts. Cell. 1985;43(2 Pt 1):405–13. https://doi.org/10.1016/0092-8674(85)90170-9.
45. Russo V, Berardinelli P, Martelli A, Di Giacinto O, Nardinocchi D, Fantasia D, et al. Expression of telomerase reverse transcriptase subunit (TERT) and telomere sizing in pig ovarian follicles. J Histochem Cytochem. 2006;54(4):443–55. https://doi.org/10.1369/jhc.4A6603.2006.
46. Tománek M, Chronowska E, Kott T, Czerneková V. Telomerase activity in pig granulosa cells proliferating and differentiating in vitro. Anim Reprod Sci. 2008;104(2–4):284–98. https://doi.org/10.1016/j.anireprosci.2007.02.003.
47. Lavranos TC, Mathis JM, Latham SE, Kalionis B, Shay JW, Rodgers RJ. Evidence for ovarian granulosa stem cells: telomerase activity and localization of the telomerase ribonucleic acid component in bovine ovarian follicles. Biol Reprod. 1999;61(2):358–66. https://doi.org/10.1095/biolreprod61.2.358.
48. Goto H, Iwata H, Takeo S, Nisinosono K, Murakami S, Monji Y, et al. Effect of bovine age on the proliferative activity, global DNA methylation, relative telomere length and telomerase activity of granulosa cells. Zygote. 2013;21(3):256–64. https://doi.org/10.1017/S0967199411000499.
49. Claude E, de Lhoneux G, Pierreux CE, Marbaix E, de Ville Goyet M, Boulanger C, et al. Detection of alternative lengthening of telomeres mechanism on tumor sections. Mol Biomed. 2021;2(1):32. https://doi.org/10.1186/s43556-021-00055-y.
50. Wright WE, Piatyszek MA, Rainey WE, Byrd W, Shay JW. Telomerase activity in human germline and embryonic tissues and cells. Dev Genet. 1996;18(2):173–9. https://doi.org/10.1002/(SICI)1520-6408(1996)18:2%3c173::AID-DVG10%3e3.0.CO;2-3.